Ecological Processes
a SpringerOpen Journal

RESEARCH Open Access

Spatial variation of net radiation and its contribution to energy balance closures in grassland ecosystems

Changliang Shao[1,2], Linghao Li[2], Gang Dong[3] and Jiquan Chen[1,2*]

Abstract

Introduction: Low energy balance closure (EBC) at a particular eddy-covariance flux site has increased the uncertainties of carbon, water, and energy measurements and has thus hampered the urgent research of scaling up and modeling analyses through site combinations in regional or global flux networks.

Methods: A series of manipulative experiments were conducted in this study to explore the role of net radiation (R_n) in the EBC in relation to spatial variability of vegetation characteristics, source area, and sensor type in three sites of the Inner Mongolian grassland of northern China.

Results: At all three sites, the residual fluxes of EBC peaked consistently at 110 W m^{-2}. The spatial variability in net radiation was 19 W m^{-2} (5% of R_n) during the day and 7 W m^{-2} (16%) at night, with an average of 13 W m^{-2} (11%) from eight plot measurements across the three sites. Large area measurements of R_n significantly increased by 9 W m^{-2} during the day and decreased by 4 W m^{-2} at night in the unclipped treatments. Net radiation decreased by 25 W m^{-2} (6% of R_n) at midday and 81 MJ m^{-2} (6%) during a growing season with heavier regular clipping than that in unclipped treatments. The R_n was lower by 11–21 W m^{-2} (~20–40% of R_n) measured by CNR1 than by Q7.1 at night, while there was only 6 W m^{-2} (~1–2% of R_n) difference during the daytime between these two types of commonly used net radiometers.

Conclusions: Overall, the inclusion of the uncertainty in available energy accounted for 65% of the ~110 W m^{-2} shortfalls in the lack of closure. Clearly, the unclosed energy balance at these three grassland sites remains significant, with unexplored mechanisms for future research.

Keywords: Inner Mongolia; Eddy-covariance; Energy balance closure; Net radiation; Spatial variability; Typical steppe

Introduction

The energy balance of the terrestrial surface can be expressed by the first law of thermodynamics, which dictates conservation of energy as:

$$R_n = H + LE + G + Q + \varepsilon \quad (1)$$

where R_n is the net radiation, H is the sensible heat flux, LE is the latent heat flux, G is the soil heat flux, Q is the sum of other heat fluxes on the surface (plants, water, etc.) with a small fraction converted to chemical energy through photosynthesis, and ε is any residual flux associated with errors. In grasslands, Q flux is relatively minor due to low and often neglected vegetation mass. If Q is small enough to ignore at a study site, the residual flux ($\varepsilon = R_n - H - LE - G$) should approximate to zero.

In-depth investigations on the energy balance and energy balance closure (EBC) of terrestrial ecosystems have been extensively revisited since the 2000s with rapid increases in the direct measurements of net exchanges of carbon and water using the eddy-covariance (EC) flux tower technology, in which the EBC plays a critical role in assessing the quality of flux measurements (Foken 2008; Oncley et al. 2007). Within the FLUXNET (http://www.fluxnet.ornl.gov/fluxnet/index.cfm) community, the EBC is considered a key indicator for evaluating the flux data quality of EC

* Correspondence: jiquan.chen@utoledo.edu
[1]Department of Environmental Sciences, University of Toledo, Toledo, OH 43606, USA
[2]Key Laboratory of Vegetation and Environmental Change, Institute of Botany, The Chinese Academy of Sciences, Beijing 100093, China
Full list of author information is available at the end of the article

measurements (Baldocchi et al. 1996; Goulden et al. 1996; Mauder and Foken 2006; Wilson et al. 2002). The low EBC (i.e., higher portion of missing energy) triggers suspicions that trace gases are not being adequately measured. This would consequently hamper the use of flux data for model validations and/or up-scaling exercises (Turnipseed et al. 2002; Wilson et al. 2002). For example, Wilson et al. (2002) reported that the magnitudes of both CO_2 uptake and respiration were underestimated when the energy imbalance was greater. Similarly, the amount of missing energy correlated negatively with the Bowen ratio (Chen et al. 2004), suggesting that the turbulent flux measurement had an error when the EBC was low.

The energy closure problem is frequently related to low turbulent energy and high available energy ($H + LE < R_n - G$), potentially due to underestimation of the turbulent energy and/or overestimation of the available energy. Foken (2008), in a review of the EBC problems, reported that the residuals of the EBC in daytime varied from 50–300 W m^{-2}, suggesting that available energy could be 30% higher than turbulent energy (Wilson et al. 2002). In recent years, numerous efforts have been made to explain the specific reasons for the EBCs at diverse flux measurement sites (Oliphant et al. 2004; Sanchez et al. 2010). Yet, no universally valid theories for the underlying mechanisms have been accepted by the community. Herein, we describe the use of a net radiometer with sufficient replications and field installations among the many reasons for conducting this EBC study.

Inadequate spatial sampling of R_n, especially when patchy vegetation and complex terrains exist, has been examined as another possible reason for EBC issues (Malhi et al. 2004; Schmid 1997). An EC site is conventionally selected to meet the theoretical needs of a large, homogeneous, and flat landscape. While turbulent energy components (i.e., sensible and latent heat fluxes) have a footprint of an entire ecosystem (normally, 50–100 sensor heights in all directions) (Chen et al. 2004), net radiation and soil heat fluxes are sampled with a much smaller footprint, with about 100 m^2 for R_n and 10^{-4} m^2 for G. These mismatched measurement footprints would not be issues when the spatial variations of vegetation, soil, and topography are minimal (Schmid 1997); however, such ideal conditions rarely exist. To improve the EBC, one solution is to increase the sampling numbers of R_n and G (i.e., increasing the measurement footprint) within the larger footprint of the turbulent footprints (Schmid 1997; Shao et al. 2008).

This paper investigates how spatial variability in R_n affects EBCs through a detailed analysis of vegetation characteristics and source area effects. Measurements for this study were conducted at three experimental sites in Inner Mongolia along temperature and water gradients to produce more general results/conclusions. Three specific questions will be answered through inter-/intra-site comparisons and manipulative experiments: i) What is the magnitude of the spatial variability in R_n at the three EC measurement sites? ii) What are the potential causes of R_n variation within and between our sites? iii) What are the contributions of R_n to EBC at these sites due to its spatial variation caused by heterogeneous vegetation? To seek the answers, we designed three experiments in a typical grassland type of Inner Mongolia and applied a mobile energy flux measurement system, which consists of nine net radiometers and other meteorological sensors with three eddy flux towers to record spatially independent R_n and associated surface properties (e.g., vegetation and soil). We specifically hypothesize that the heterogeneity of vegetation structure plays an important role in the EBC due to its direct alterations of the outgoing (or reflectance) of short- and long-wave radiation that determine the magnitude of net radiation.

Methods

Site descriptions

Experiment 1 was designed to measure R_n at three EC measurement sites: Duolun (site I), Xilinhot (site II), and Dongwu (site III) of Inner Mongolia, northern China, during the growing season of 2006. Experiments 2 and 3 were conducted at site I during the growing season of 2007 in a manipulative plot that is approximately 1,000 m south of the EC tower (Table 1).

Site I (42° 02′ N, 116° 17′ E, 1,380 m asl) involved in Experiments 1–3 was located at the Shisanlitan Grassland Ecosystem Restoration Research Station in Duolun County, a semiarid agriculture-pasture transition area in southeastern Inner Mongolia. The site has a distinct continental climate with a mean annual relative humidity of 61% and a mean annual precipitation of 399 mm (375 mm in 2007), which falls primarily from May to October. The mean

Table 1 Net radiometers and their deployments in the three experiments in this study

Experiment		Period of measurement	Sensor used	Height
1	Site I	Jul 9–29, 2006	Eight Q7.1 s; one CNR1	Q7.1 2 m; CNR1 4 m
	Site II	Jul 31–Aug 20, 2006	Eight Q7.1 s; one CNR1	Q7.1 2 m; CNR1 4 m
	Site III	Aug 21–Sept 15, 2006	Eight Q7.1 s; one CNR1	Q7.1 2 m; CNR1 3.5 m
2		Jun 3–30; July 26–Oct 31, 2007	Nine Q7.1 s	0.3–0.5 m above the canopy
3		Jul 13–21, 2007	Six Q7.1 s	Small 0.5 m; large 1.5 m

annual temperature is 3.3°C, with a mean monthly temperature ranging from −15.9°C in January to 19.9°C in July (1990–2004). Summers are relatively damp and warm while winters are rather cold, dry, and windy. The study site was flat with relatively homogenous vegetation within the landscape. The experimental manipulations were conducted in the *Stipa krylovii* grassland, which is the most dominant vegetation type in the region. The soils are chestnut soils and below 0.4 m, there is a mixture of sandy soil and gravel. The site has been fenced since 2001 to prevent large herbivores, such as cattle and sheep, from grazing on the grassland, as had previously occurred. The dominant species include *Stipa krylovii*, *Artemisia frigida*, and *Potentilla acaulis*.

Site II (43° 33′ N, 116° 40′ E, 1,120 m asl) is at the Inner Mongolian Grassland Ecosystem Research Station of the Chinese Ecosystem Research Network. The site is exposed to a temperate, semi-arid continental climate with a mean annual temperature of 2.6°C and mean monthly temperatures ranging from −18.8°C in January to 21.2°C in July over the past 30 years. The mean annual precipitation is 350 mm. The dominant wind direction is northwest with an average wind velocity of 3.4 m s^{-1} during the sampling period. Chestnut and dark chestnut soils are the zonal soil types (Chen et al. 2005). The dominant plant species are two perennial grass species, *Leymus chinensis* and *Stipa grandis*.

At site III (45° 33′ N, 116° 59′ E, 840 m asl), the mean annual precipitation is 259 mm and the mean annual temperature is 1.4°C, with mean monthly temperatures ranging from −20.8°C in January to 21.1°C in July over the past 30 years. The growing season usually begins in mid-May and ends in late September. The mean wind direction is southwesterly from June 1 to September 30, with an average wind velocity of 3.1 m s^{-1} during the sampling period. The experimental plot is very flat and homogenous with degraded typical grasslands. The dominant species are *Salsola collina* and *Leymus chinensis*. For further site information, see Shao et al. (2008).

Experiment 1: Spatial variability of R_n within the EC footprints

All of the EBC terms in Eq. (1) were directly measured at each of the EC towers (Zhang et al. 2007). R_n was measured by four-component net radiometers CNR1 (Kipp & Zonen, Delft, the Netherlands). The open path EC tower included a fast response three-dimensional ultrasonic anemometer (CSAT3, Campbell Scientific Inc. (CSI), Logan, UT, USA) installed 3 m above the ground and a LI7500 InfraRed Gas Analyzer (IRGA, LiCor Inc., Lincoln, NE, USA) to obtain the *LE* and *H*. We arbitrarily laid out a 50 × 50 m^2 plot around the three EC towers to install the mobile energy balance (EB) system, which consists of eight stations in an orthogonal layout with 12.5 m intervals in the four cardinal directions. That is, two stations were installed at distances of 12.5 and 25 m from the center point in each direction. Each station was equipped with a Q7.1 net radiometer (Radiation Energy Balance System (REBS), Seattle, WA, USA) mounted 2.0 m above the ground, two heat flux transducers (HFT3.1, REBS) buried at 0.025 m depth to measure soil heat flux (G_0), and one custom-made T-type copper-constantan thermocouple to measure soil temperature at 0.05 m depth (T_s). The mobile EB system also included four water content reflectometers (model CS616, CSI) in the four directions at a depth of 0.025 m (upper pole) to record soil volumetric water content (θ), and three E-type chromel-constantan thermocouples to measure soil surface temperature (T_0). Soil bulk density (ρ_b), from surface to 0.05 m depth, was measured in four replicates in each direction at each site. T_s, T_0, θ, and ρ_b were used to calculate the soil layer heat storage (S) above the two HFT3.1 s. The sum of G_0 and S is soil heat flux (G). All the Q7.1 s were corrected by using the same wind speed derived from an anemometer (05103, CSI) that was mounted at 2 m above the ground at each site. Data was collected at 10 s intervals and compiled as 30 min averages with a CR10X datalogger (CSI). The prevailing wind directions were northwest for sites I and II, and southwest for site III, with average wind velocities of 3.5, 3.4, and 3.1 m s^{-1} from June 1 to September 30 for sites I, II, and III, respectively. A footprint analysis was performed using the method of Stannard (1997, Eqn. (18), P382), showing that, at all three tower sites, approximately 99% of measured scalar fluxes originated within 500 m of the tower and approximately 97% originated with 250 m.

Experiment 2: Vegetation influence

To assess the influence of vegetation on R_n, a precision manipulative experiment initiated in 2003 near site I but outside the EC tower footprint was used. The experiment was planned in a single-factor design with five clipping treatments and five replications on the grassland: remaining shoot height 0.02 (M_2), 0.05 (M_5), 0.10 (M_{10}), 0.15 m (M_{15}), and without clipping (M_0, control). Three replicate microclimatic stations were installed in each of the M_2, M_{10}, and M_0 treatments, for a total of nine stations. Continuous measurements of micrometeorological variables began on June 3 (DOY 154) throughout the growing season, 2007. After four years of continuous clipping, the dominant species changed from heterogeneous tall-stature bunchgrass *Stipa krylovii* grassland (treatment M_0) to homogeneous short-stature semi-shrub *Artemisia frigida* grassland (treatment M_2). The cover, biomass, and biomass-per-cluster in *Stipa krylovii*, leaf area index, green biomass, height, and litter weight in the communities of M_2 plots were consistently less than those of M_{10} and M_0 plots (Table 2).

Table 2 Vegetation characteristics at growing seasonal peak time for clipping treatments where Experiments 2 and 3 were conducted

Treatment	Vegetation cover (%)	Leaf area index	Living biomass (g m^{-2})	Litter (g m^{-2})	Stand dead (g m^{-2})	Average height of vegetation (m)	Number of species
M_2	54 ± 2^a	0.34 ± 0.02^a	66 ± 8^a	48 ± 8^a	25 ± 4^a	0.04 ± 0.01^a	15 ± 1^a
M_{10}	49 ± 2^a	0.38 ± 0.02^a	76 ± 10^a	58 ± 17^a	24 ± 1^a	0.09 ± 0.01^b	14 ± 2^a
M_0	48 ± 5^a	0.48 ± 0.02^b	112 ± 7^b	130 ± 14^b	177 ± 19^b	0.23 ± 0.02^c	12 ± 1^b

M_2, M_{10}, and M_0 showed biomass removal by clipping shoots at heights of 0.02 m, 0.10 m, respectively, once a year in late August since 2003 and no clipping. Values (mean ±1 SE) designated by the same letter (^{a}, ^{b}, or ^{c}) are not significantly different at $P = 0.05$ among treatments.

The 25 10×20 m^2 plots were randomly assigned for treatment types and placed with 4 m gaps between the adjacent plots. A push mower (Yard-man 160CC, USA) was used to clip the vegetation in late-August once a year and plants were allowed to grow until the next clipping. The nine stations were distributed randomly avoiding the edge effects (Chen et al. 1992).

Experiment 3: Influence of the source area

The size of the source area under a radiometer can also be critical, since a large source area will often include more diverse land surfaces. Three paired Q7.1 net radiometers were randomly selected for July 12–20, 2007, with one Q7.1 raised to 1 m higher than the others during a four-day study period (Table 1).

The source area of a radiometer with a hemispherical windshield can be calculated as:

$$A = 1 - \left[(R/h)^2 + 1\right]^{-1} \quad (2)$$

where A is the relative contribution to the measured flux signal from a partial source area (centered below the net radiometer) of radius R for net radiometer height above the canopy of h (Stannard et al. 1994). When $R/h = \infty$, $A = 1$. In Experiment 2, as $R/h > 10$, ≈99% contributed from each of the measured clipping plots; while in Experiment 3, $R/h = 3.3$, therefore $A = 92\%$. The plot area in our study was large enough for all three experiments. Experiment 1 was conducted in the summer of 2006 with the new eight factory calibrated Q7.1 s. These Q7.1 s were moved to the three sites (I, II, and III) in turn, and then an inter-comparison was conducted before Experiments 2 and 3. At this time, nine Q7.1 s were randomly divided into three groups and operated side by side. Descriptions of net radiometer deployments of Experiments 1–3 are listed in Table 1. In addition to the factory calibration of Q7.1 at the beginning of Experiment 1, a one week field inter-comparison (Halldin and Lindroth 1992) was also conducted during Experiment 2 (Table 3).

Eddy-covariance data processing

The July to September raw 10 Hz time series data from the EC measurements were processed off-line using the EC_Processor software package (http://research.eeescience.utoledo.edu/lees/ECP/ECP.html) (Noormets et al. 2007; 2010) for sites I, II, and III, respectively, which were corrected by the double rotation method. The turbulent fluxes were adjusted for fluctuations in air density using the Webb-Pearman-Leuning expression (Webb et al. 1980). A series of data quality controls were used in the EC_Processor; for example, data quality was judged by atmospheric stability. Obvious outliers were removed, such as anomalous or spurious data that were caused by sensor malfunction, sensor maintenance, rainfall events, IRGA calibration, power failure, etc. A friction velocity u^* (Goulden et al. 1996) of <0.15 m s^{-1} was used in this study (Zhang et al. 2007). Following these quality tests, the remaining data were classified as 'good data' to be submitted for analysis. Consequently, 52%, 42%, and 40% of the July–September growing season H and LE data obtained from our EC systems of sites I, II, and III, respectively, were discarded in Experiment 1. We did not intend to gap-fill the data and only the 'good data' were used in this energy balance closure analysis.

Data analysis

We analyzed the energy balance residual and applied linear regression to explore the spatial variability in R_n contributing to EBC in Experiment 1. First, the data from 12, 16, and 17 days at sites I, II, and III, respectively, were

Table 3 One week inter-comparison between the Q7.1 net radiometers before Experiments 2 and 3 in 2007

Between[§]	OLS slope	Intercept	r^2
1, 2	0.98	−0.64	0.999
1, 3	0.99	−1.64	1.000
2, 3	1.01	−0.37	0.999
4, 5	0.99	1.53	1.000
4, 9	0.99	1.19	1.000
5, 9	1.01	−0.12	1.000
6, 7	0.98	0.76	1.000
6, 8	0.99	0.99	1.000
7, 8	1.01	0.12	1.000
Mean (SE)	0.99 (0.00)	0.20 (0.34)	1.00 (0.00)

[§]In the first column, the first value is the independent variable and the second value is dependent variable when making the linear regression; r^2 is the coefficient of determination.

compiled into 30 min averages to illustrate the residual fluxes of EBC (i.e., ε). Then, the data was examined using an ordinary least square (OLS) linear regression by relating dependent turbulence energy ($H + LE$) and independent available energy ($R_n - G$). The mean values of the 30 min R_n and G from eight replicated measurements were calculated at each site. The mean values of R_n were used to compare the closures resulting from Q7.1 with those from CNR1 at the EC towers. The maximum and minimum values were used to illustrate the spatial variability of R_n and its contribution to the EBC. The mean values of G from sixteen replications were used to calculate the EBC. Rainy days were deliberately avoided, because the turbulent flux instruments would not work well at those times. For Experiments 2 and 3, all the 30 min experimental periods data were also integrated and examined on a diurnal scale. The paired T-test (SPSS 13.0 software) was used to analyze R_n deployment by height to find its contribution to the EBC. R_n differences among treatments/plots were used to examine the influences of vegetation and source area.

Results

Spatial variability of R_n

The ε averaged 19 W m^{-2} (i.e., 5% of R_n) during the day and 7 W m^{-2} (16%) at night across the three sites due to the spatial variability in R_n (Table 4 and Figure 1). The daytime ε were 48, 68, and 67 W m^{-2} due to the maximum R_n for sites I, II, and III, respectively, and 33, 48, and 47 W m^{-2} due to the minimum R_n (Table 4 and Figure 1). Altogether, the spatial variability in R_n contributing to the EBC was approximately 13 W m^{-2} or 11% of the daily mean R_n (Table 4). A 4% OLS slope difference (0.88 and 0.92) was found from the replicated R_n sampling (i.e., spatial variability). The OLS slopes for sites I, II, and III were 0.97, 0.93, and 0.86 for the minimum R_n, respectively, and 0.95, 0.89, and 0.81 for the maximum R_n. The wet site (i.e., site I) had the highest OLS slopes for both day and night.

The daytime ε was higher than that at night, but the portion to R_n was greater at night in all three sites. The daytime ε was 33 to 68 W m^{-2} with the portion to R_n being 3% to 5%, while the nighttime ε was −7 to 7 W m^{-2} with the portion to R_n being 14% to 20% (Table 4).

Sensor influence

The R_n values from the Q7.1 and CNR1 net radiometers were different and varied by time. The residual fluxes of the EBC (i.e., ε) were similar between the two radiometers during the day but higher (less negative) from the Q7.1 at night in all three sites (Figure 2). In the daytime, especially from 9:00 to 15:00 h, only 6 W m^{-2} (~1% of R_n) difference among the three sites was found. However, larger differences appeared at night, reaching up to 21 W m^{-2} (~40% of R_n) at sites I and III, whereas at site II, the difference was 11 W m^{-2} (~20% of R_n).

The OLS linear regression showed similar results, with 10% OLS slope difference for the Q7.1 measurements (0.91) and the CNR1 (0.81) across the three sites (Figure 3). The Q7.1 provided an OLS slope of 0.84 to 0.97, while the CNR1 had slopes of 0.73 to 0.88.

Vegetation influence

With an increase in clipping intensity, R_n decreased during most of the daytime throughout the growing season (Figure 4). At midday, the average R_n values were 413, 395, and 388 W m^{-2} for the M_0, M_{10}, and M_2 treatments over the growing season, respectively. The R_n in M_2 was nearly 6% lower than in M_0 treatments both at midday and by daily total. Over the growing season, the total R_n were 1409, 1331, and 1328 MJ m^{-2} for M_0, M_{10}, and M_2, respectively, i.e., in the heavily mowed treatment (M_2) decreased by another 6% (or about 81 MJ m^{-2}) as compared to the reference.

Source area influence

The size of observed R_n source, changed by deploying Q7.1 at different heights, did not show a significant influence in M_2 and M_{10}, but did in M_0 treatments (Figures 5 and 6). With M_0 treatment, the R_n difference was 9 W m^{-2} during the day (9:00–15:00 h, P <0.0001) and 4 W m^{-2} at night (21:00–3:00 h) between the two heights. In M_2 and M_{10} treatments, however, the R_n differences were generally <2 W m^{-2} throughout the day.

Discussion

Inter-comparison

The primary focus of this study was to seek potential sources of missing R_n energy within the EBC at multiple

Table 4 Energy balance closure residuals (ε, W m^{-2}) resulted from the spatial variability in R_n at the three grassland sites (I, II, and III)

Site	Midday	Midnight	Day[§]	Night[§]	Day and night
I	38 to 54 (3)	−10 to −1 (20)	33 to 48 (3)	−7 to 2 (20)	13 to 25 (12)
II	65 to 87 (5)	1 to 7 (13)	48 to 68 (5)	1 to 7 (14)	25 to 38 (9)
III	57 to 80 (6)	−11 to −4 (16)	47 to 67 (6)	−6 to 1 (15)	20 to 34 (11)
Average	20 (5)	7 (16)	19 (5)	7 (16)	13 (11)

Average row shows the mean ε spatial variability of the three sites. The number in brackets is the percentage of ε/R_n; [§]Day and night refer to 9:00–15:00 and 21:00–3:00 h, respectively. Data are derived from Experiment 1.

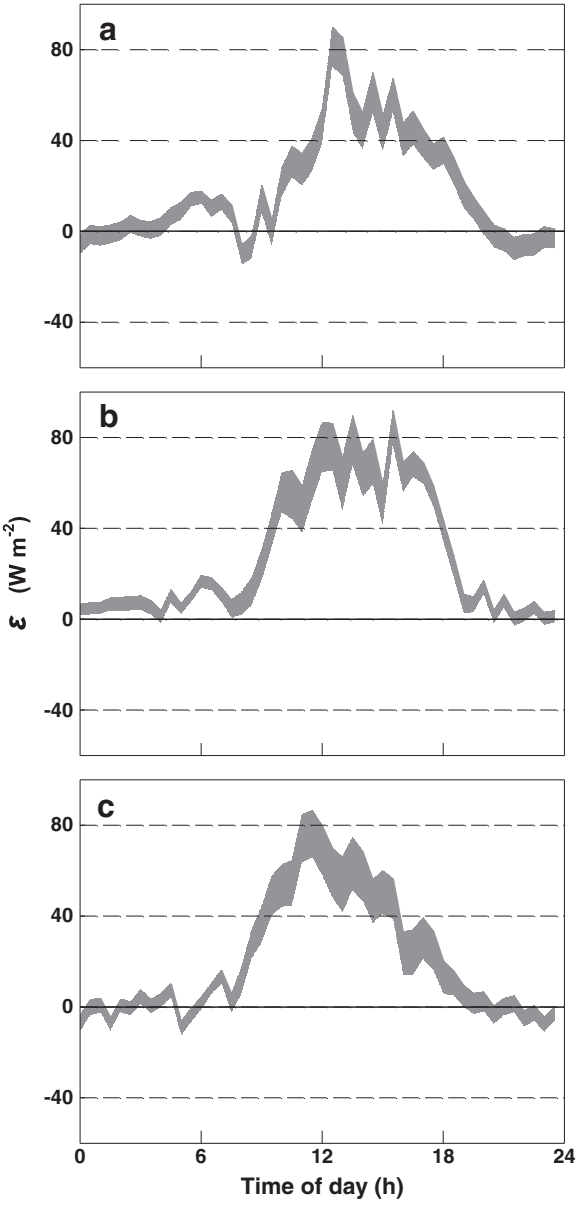

Figure 1 Uncertainties in energy balance closure residuals (ε) due to spatial variability in R_n. The upper and lower bounds of the gray band derived from the maximum and minimum R_n of the eight treatments, respectively. Site I **(a)**, II **(b)**, and III **(c)**. Data are derived from Experiment 1.

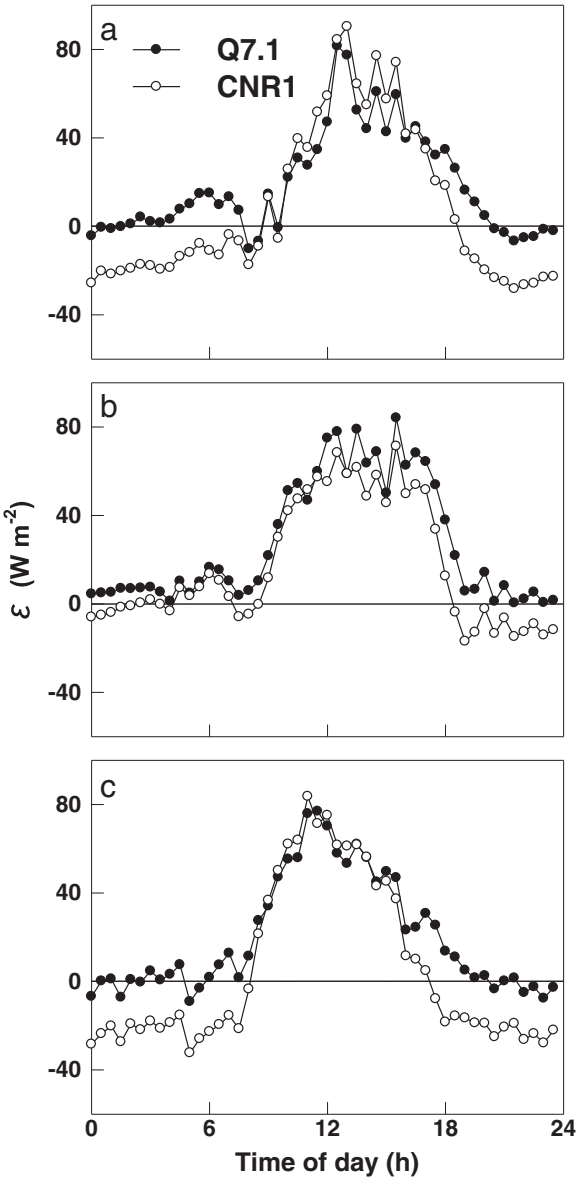

Figure 2 Energy balance closure residuals (ε) derived from Q7.1 and CNR1 measurements in R_n. Site I **(a)**, II **(b)**, and III **(c)**. Data are derived from Experiment 1; 30 min averages data from 12, 16, and 17 days at sites I, II, and III, respectively, were compiled into a one-day scale, the same as in Figure 1.

sites where vegetation structure had been manipulated. In the last 15 years, much has been done to increase the accuracy of the radiation measurements (Foken 2008; Kohsiek et al. 2007; Wilson et al. 2002). The regression slope of the comparisons remained constant over the sampling period for the three treatments, suggesting that the Q7.1 is a stable sensor (Table 3). Further evidence showing small differences (Figures 5 and 6) at the M_2 among Q7.1 radiometers (0.5 W m^{-2} during 9:00–15:00 h and 1 W m^{-2} between 21:00–3:00 h) are likely due to the more homogeneous vegetation. Clearly, the error related with the different Q7.1 could be reduced with good maintenance. However, in the early evening, the Q7.1 can produce occasional spikes (Figures 5 and 6).

Spatial variability of R_n and the EBC

The spatial variability of the R_n measured from multiple Q7.1 sensors was 19 W m^{-2} (5% of R_n) during the day and 7 W m^{-2} (16%) at night, with a daily average of 13 W m^{-2} (11%) or a 4% OLS slope. This variability might be due to the differences in vegetation structure, soil

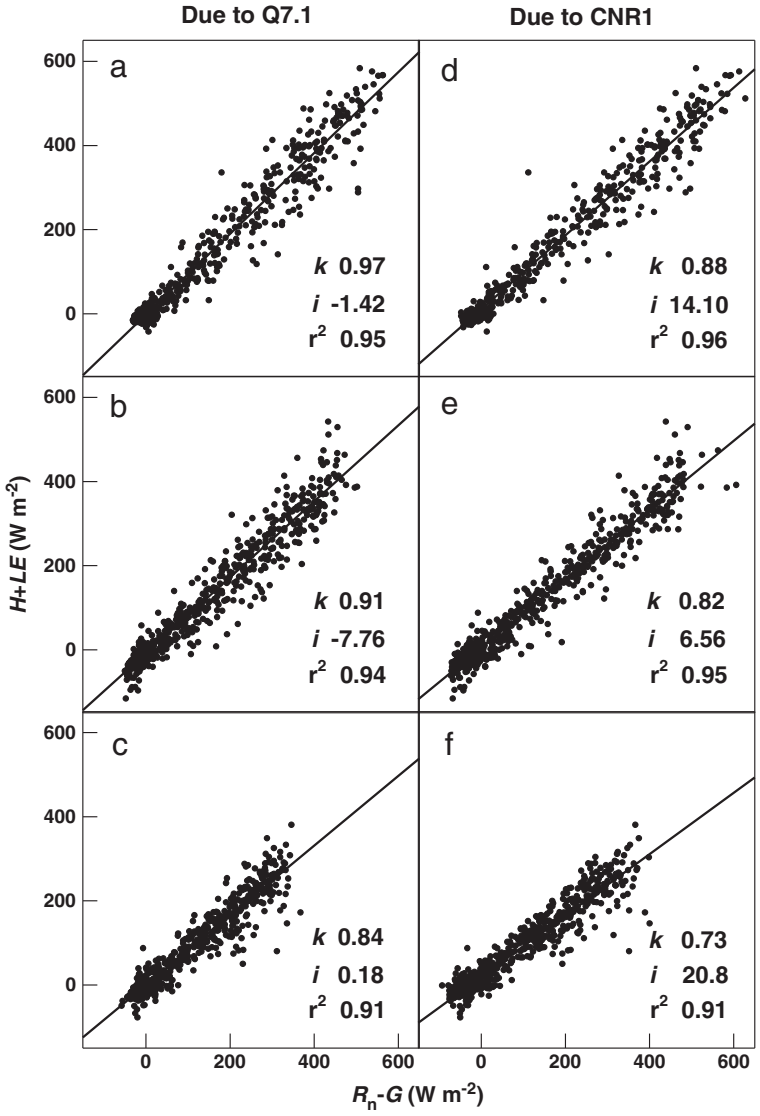

Figure 3 Comparisons of 30 min values of turbulent ($H + LE$) vs. available energy ($R_n - G$). Data derived from Q7.1 "(Left)" and CNR1 "(Right)" determined R_n with the ordinary least square (OLS) linear regression equation of $(H + LE) = k\,(R_n - G) + i$ (k, slope, i intercept, coefficient of determination, r^2 are also shown). The solid line shows OLS linear regression fit. Site I **(a**, **d)**, II **(b**, **e)**, and III **(c**, **f)**. Data are derived from Experiment 1.

characteristics, and microclimates among the eight plots at each site. However, the spatial variability in available energy is still smaller to account for the lack of closure. The turbulent flux is systematically lower by 110 W m^{-2} at peak time than the available energy (Figures 1 and 2). The uncertainty in R_n could contribute to a systematic error of about 20 W m^{-2} (21 ± 3 W m^{-2} at midday across the three sites), or 5% of R_n which is in consistent with the report by Twine et al. (2000) of 6% of midday and mid-season R_n at a grass site in Oklahoma. The uncertainty in soil heat flux could contribute another 50 W m^{-2} (53 ± 11 W m^{-2}) of error to the available energy (Shao et al. 2008). Altogether, the inclusion of the uncertainty in available energy accounted for about 65% of the 110 W m^{-2} (111 ± 10 W m^{-2}) shortfall in the lack of closure. Clearly, the unclosed energy balance at these three grassland sites remains real and there remain unexplored mechanisms. Yet, it is unlikely that improper measurement of R_n during the daytime is responsible for the energy imbalance because both CNR1 and Q7.1 were in relative accordance during the course of the study (see also Turnipseed et al. 2002).

We designed a large scale plot (50 × 50 m^2) with 8 Q7.1 s and 16 soil heat flux plates to quantify the spatial variability in R_n and G approximately to match with the source area with H and LE. The mean R_n and G stood reasonably well for the large-scale realities. There still existed 47 ± 16, 50 ± 13, and 70 ± 15 W m^{-2} of the energy

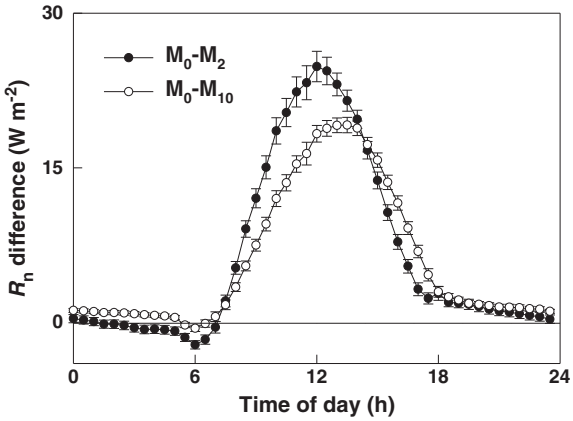

Figure 4 Half-hourly differences of R_n between unclipped control and clipped treatments. (M_0–M_2) means shoots clipped at 0.02 m and (M_0–M_{10}) at 0.10 m. Each value is the average of growing season from 3 June to 31 October, 2007. Data are derived from Experiment 2.

balance at midday that could not be explained at sites I, II, and III, respectively. Even with all of the spatial uncertainties included, an imbalance of ~20 W m^{-2} still existed, perhaps due to other instrumental, operational, and flow based errors (Finnigan 2008). Examples of these errors are *H*, *LE*, or both of the turbulent fluxes at either low- and/or high-frequency and mean vertical or horizontal advection of scalar quantities. Moore et al. (1986) and Massman (2000) reported that the low and/or high frequency spectral losses were another reason from turbulence measurements caused the imbalance of energy balances. In the literature, flux loss was typically 5% to 10% for sensible and latent heat fluxes (Moore 1986). In our three sites, the average midday $H + LE$ was nearly 300 to 400 W m^{-2}, so the spectral loss perhaps reached 15 to 40 W m^{-2}, which is also important in EBC. Gash and Dolman (2003) and van der Molen et al. (2004) argued that turbulence energy from sonic anemometer (co)sine errors was a potential source, while Aubinet et al. (2000) and Foken et al. (2001) pointed out that the time lag among different energy flux measurements need to be considered. Twine et al. (2000) also calculated that the uncertainties from R_n and *G* could only account for half of their imbalance 130 W m^{-2} in grassland at midday.

Sensor differences

The domes on the Q7.1 sensor might have a low thermal transmissivity resulting in underestimated incident thermal sky radiation (Twine et al. 2000). Additionally, the CNR1 measured a wider spectrum of wavelengths than Q7.1,

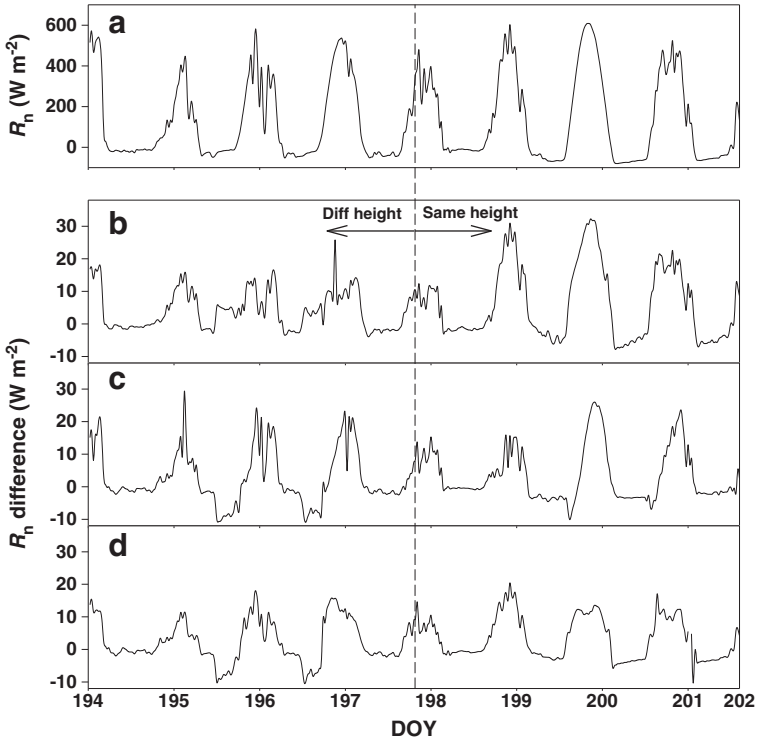

Figure 5 Net radiometer deployment heights vs. R_n results (half-hourly data integrated into a diurnal scale). Diff height means R_n differences between the two Q7.1 s deployed above the canopy by 0.5 and 1.5 m, respectively. Same height means both of the two Q7.1 s deployed above the canopy by 0.5 m. M_0, M_{10}, and M_2 refer to unclipped areas and areas with shoots clipped at 0.10 and 0.02 m at the end of each growing season, respectively. Data are derived from Experiment 3.

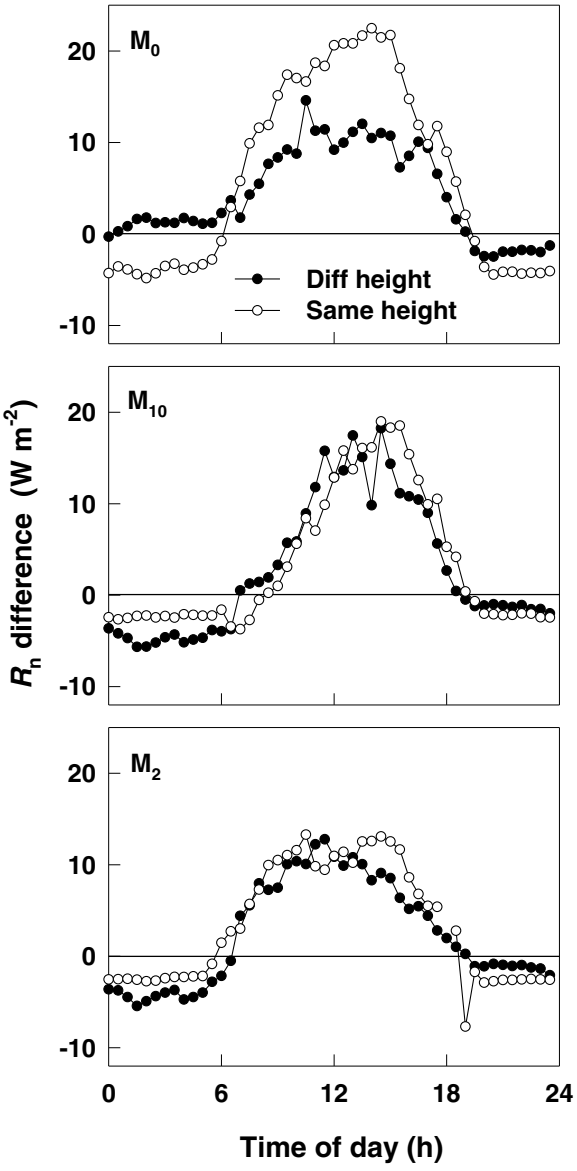

Figure 6 Net radiometer deployment heights vs. R_n results with Figure 5 half-hourly data integrated into a diurnal scale.

which could also introduce additional bias, particularly in the nighttime. There is no doubt that this discrepancy would lead to a large variation in ε at night. In this study, the R_n of the CNR1 were significantly lower (10 to 20 W m^{-2}) at night than those of the Q7.1, with the OLS slope varying approximately 4% (Figure 2). Kohsiek et al. (2007) compared these two types of radiometer and found a similar difference at night (15 W m^{-2}). In our study, the regression slope remained constant during the study period at all three sites (1.04 ± 0.02), using the value of Q7.1 as the independent variable. This suggests that the calibrations of the two instrument types remained constant (Turnipseed et al. 2002), with regression slopes of 1.00 ± 0.01 in the daytime (9:00–15:00 h) and 1.31 ± 0.07 at night (21:00–3:00 h). Nighttime measurements of R_n, however, showed substantial discrepancies between the two sensors – close to 1.25 reported by Turnipseed et al. (2002) in a forest where the authors suspected as an error in the 'long-wavelength measurement of one or both radiometers'. Other authors (Halldin and Lindroth 1992; Hodges and Smith 1997; Oncley et al. 2007) also noticed the discrepancies between different instruments. The magnitudes of nocturnal turbulent heat fluxes are typically underestimated with the EC method, as turbulence is generally low. The underestimation (less negative) of nocturnal R_n value from Q7.1 would further increase EBC. Thus, this difference must be taken into account when comparing and calculating EBC among or within sites.

The different EBC could also occur at different time scales. On a half-hourly scale, for example at site I, it showed the same daytime EBC between CNR1 and Q7.1, while the ε value determined by the Q7.1 was closer to zero at night. Therefore, we conclude that Q7.1 measurements provided much 'better closure' (Figure 2a) because of the underestimation of the magnitude of R_n with the Q7.1 during night-time. However, on a daily scale, it seemed that CNR1 provided better measurements. On a typical day (July 11), the daily imbalance yielded 1.44 MJ $m^{-2}d^{-1}$ using Q7.1 but only 0.63 MJ $m^{-2}d^{-1}$ using CNR1.

Due to the difference between the Q7.1 and CNR1, a method in comparing the EBCs within and among sites at a specific period from 9:00 to 15:00 h during the daytime would be useful to provide definite results both in residual and OLS regression methods. This is because during this period, the sensors (net radiometer, sensible and latent heat measurements) usually worked in their best conditions (e.g., high friction velocity). Different kinds of gap-filling strategies (Falge et al. 2001) in *H* and *LE* usually impede further EBC analysis. Furthermore, in the early morning and evening when net radiation is changing most rapidly, the magnitude of storage heat in the soil, air, and biomass can approach that of R_n (Moore and Fisch 1986). In addition, toward midday, the storage heat is less important (McCaughey 1982). Using this method, the effect of differences between instruments would be partially avoided.

Potential causes of R_n measurements for non-closure

In addition to the spatial variability resulting from vegetation, radiometer type and source area could also be responsible for inaccurate R_n measurements. In the unclipped plot, R_n might be higher due to a lower *albedo* in comparison to the clipped one (Li et al. 2006). The Student's *t*-test, with a 0.05 level of significance, was used in previous studies to examine the differences between samples from the different clipping treatments (Shao et al. 2012). The maximum contrast in vegetation was found between sample

treatments M_0 and M_2 with the latter having less leaf area index and green biomass (Table 2). This explained the 6% difference in R_n that was recorded in Experiment 2 (Figure 4), and also the peak difference of ~10 to 20 W m^{-2} between M_0 and M_2 in Experiment 3 (Figure 6) in our grassland sites. Similarly, a higher R_n in grazed compared to ungrazed management in desert steppe was also observed (Shao et al. 2013). Further, the reduced R_n energy input from the atmosphere by clipping or grazing land-use types has important implications for global warming studies and ecosystem modeling.

The source area experiment indicated that Q7.1 deployment needs to be high enough to record reliable R_n, especially under heterogeneous surface. The typical deployment height of 1.5 to 2.0 m seemed to be inadequate to integrate across vegetation heterogeneity (Stannard et al. 1994). An error would appear with low installation height of radiometers because the sensor could not receive the representative long- and short-wave reflections from the surface. However, Lloyd et al. (1997) pointed out that as the height of the net radiometer increases, the measurement would be degraded by long-wave losses in the air layer between the surface and the measurement height.

From Figure 3, comparing sites II and III with I, when the *LE* was larger the energy closure was better. We speculate that the mismatch between the energy fluxes (Shao et al. 2008) and the underestimated *LE* (Dugas et al. 1991) at our arid sites may be responsible for this imbalance. Since sensible heat fluxes between both systems compared better than latent heat fluxes (Schlesinger et al. 1996), we agree with the view that the instrument could cause bigger error when *LE* was lower (Stannard et al. 1994); this point needs to be studied further. The closure issue becomes even more important upon consideration of the long-term water balance. Twine et al. (2000) summed over a period of 15 days from 4 EC systems and drew a conclusion that evapotranspiration would be significantly overestimated by calculating *LE* as the residual of the energy budget; this is also supported by others (Dugas et al. 1991; Kampf et al. 2005; Nie et al. 1992). Thus, in our study, it is a risk to use the EC residual method to estimate *LE* since there were more uncertainties from R_n, *G*, *S*, and other heat sinks, especially when *LE* is smaller or under a certain spatial scale. This coincided with previous studies (Twine et al. 2000; Wilson et al. 2002) indicating that each flux should be analyzed separately.

Conclusions

Net radiation contributions to the EBC were examined through three experiments in grassland where EC towers had been installed since 2005. A large scale plot (50 × 50 m^2) with 8 Q7.1 s and 16 soil heat flux plates was firstly designed to quantify the spatial variability in R_n and *G* approximately to match with the source area with *H* and *LE*. The spatial variabilities of vegetation, source area, and sensor type in grassland played critical roles in the EBC of our study sites. Despite the fact that net radiation (estimated too high) and soil heat (estimated too low) could not be excluded, the spatial variability quantity in net radiation is less than that in soil heat flux, and the sum of these two energy fluxes (i.e., available energy) accounted for 65% of the missing energy. The other portion of missing energy remains at large, nearly 40 W m^{-2} at the daytime peak time. More effort under different conditions (e.g., winter, spring, and fall when different phenological vegetation exist, different weather conditions, and long temporal scales) must be made in a similar way to reach a comprehensive understanding of EBC. For example, from this study, we noticed also that the EBC was better under conditions of higher soil moisture, higher *LE*, higher vegetation cover, lower *H*, and lower latitude. However, further work needs to be performed to systematically explore the mechanisms or empirical relationships.

Abbreviations

EB: Energy balance; EBC: Energy balance closure; EC: Eddy-covariance; *G*: Soil heat flux; *H*: Sensible heat flux; OLS: Ordinary least square; *Q*: Sum of other heat fluxes on the surface; R_n: Net radiation; *S*: Soil layer heat storage; *T*: Soil surface temperature; ε: Residual flux associated with errors; θ: Volumetric water content; ρ_b: Soil bulk density.

Competing interests

The authors declare that they have no competing interests.

Authors' contributions

CLS, JQC, and LHL conceived and designed the experiments. CLS and GD performed the experiments. CLS and JQC analyzed the data and wrote the paper. JQC and LHL contributed the reagents/materials/analysis tools. All authors read and approved the final manuscript.

Acknowledgements

This study was supported by the Natural Science Foundation of China (31170454, 31229001, 31130202), the State Key Basic Research Development Program of China (2013CB956600), the NASA-NEWS Program (NN-H-04-Z-YS-005-N), and the USCCC. We would like to thank Asko Noormets for "EC processor" software, and Xin Li and Zhichun Yan for their assistance in fieldwork. We greatly appreciate the editorial support from Valerie Pinkerton, Lisa Delp Taylor, and Alona Gutman.

Author details

[1]Department of Environmental Sciences, University of Toledo, Toledo, OH 43606, USA. [2]Key Laboratory of Vegetation and Environmental Change, Institute of Botany, The Chinese Academy of Sciences, Beijing 100093, China. [3]School of Life Science, Shanxi University, Taiyuan 030006, China.

Received: 8 January 2014 Accepted: 20 February 2014
Published: 3 March 2014

References

Aubinet M, Grelle A, Ibrom A, Rannik U, Moncrieff J, Foken T, Kowalski AS, Martin PH, Berbigier P, Bernhofer C, Clement R, Elbers J, Granier A, Grunwald T, Morgenstern K, Pilegaard K, Rebmann C, Snijders W, Valentini R, Vesala T (2000) Estimates of the annual net carbon and water exchange of forests: The EUROFLUX methodology. Adv Ecol Res 30:113–175

Baldocchi DD, Valentini R, Running S, Oechel W, Dahlman R (1996) Strategies for measuring and modelling carbon dioxide and water vapour fluxes over terrestrial ecosystems. Global Change Biol 2(3):159–168

Chen JQ, Franklin JF, Spies TA (1992) Vegetation responses to edge environments in old-growth Douglas-Fir forests. Ecol Appl 2(4):387–396

Chen JQ, Paw U, Ustin SL, Suchanek TH, Bond BJ, Brosofske KD, Falk M (2004) Net ecosystem exchanges of carbon, water, and energy in young and old-growth Douglas-fir forests. Ecosystems 7(5):534–544

Chen SP, Bai YF, Zhang LX, Han XG (2005) Comparing physiological responses of two dominant grass species to nitrogen addition in Xilin River Basin of China. Environ Exp Bot 53(1):65–75

Dugas WA, Fritschen LJ, Gay LW, Held AA, Matthias AD, Reicosky DC, Steduto P, Steiner JL (1991) Bowen-ratio, eddy-correlation, and portable chamber measurements of sensible and latent-heat flux over irrigated spring wheat. Agric For Meteorol 56(1–2):1–20

Falge E, Baldocchi D, Olson R, Anthoni P, Aubinet M, Bernhofer C, Burba G, Ceulemans G, Clement R, Dolman H, Granier A, Gross P, Grunwald T, Hollinger D, Jensen NO, Katul G, Keronen P, Kowalski A, Lai CT, Law BE, Meyers T, Moncrieff J, Moors E, Munger JW, Pilegaard K, Rannik U, Rebmann C, Suyker A, Tenhunen J, Tu K, Verma S, Vesala T, Wilson K, Wofsy S (2001) Gap filling strategies for long term energy flux data sets. Agric For Meteorol 107(1):71–77

Finnigan J (2008) An introduction to flux measurements in difficult conditions. Ecol Appl 18(6):1340–1350

Foken T (2008) The energy balance closure problem: an overview. Ecol Appl 18(6):1351–1367

Foken T, Wichura B, Klemm O, Gerchau J, Winterhalter M, Weidinger T (2001) Micrometeorological measurements during the total solar eclipse of August 11, 1999. Meteorol Z 10(3):171–178

Gash JHC, Dolman AJ (2003) Sonic anemometer (co)sine response and flux measurement I. The potential for (co)sine error to affect sonic anemometer-based flux measurements. Agric For Meteorol 119(3–4):195–207

Goulden ML, Munger JW, Fan SM, Daube BC, Wofsy SC (1996) Measurements of carbon sequestration by long-term eddy covariance: methods and a critical evaluation of accuracy. Global Change Biol 2(3):169–182

Halldin S, Lindroth A (1992) Errors in net radiometry – comparison and evaluation of 6 radiometer designs. J Atmos Ocean Technol 9(6):762–783

Hodges GB, Smith EA (1997) Intercalibration, objective analysis, intercomparison and synthesis of BOREAS surface net radiation measurements. J Geophys Res (A Atmospheres) 102(D24):28885–28900

Kampf SK, Tyler SW, Ortiz CA, Munoz JF, Adkins PL (2005) Evaporation and land surface energy budget at the Salar de Atacama, Northern Chile. J Hydrol 310(1–4):236–252

Kohsiek W, Liebethal C, Foken T, Vogt R, Oncley SP, Bernhofer C, Debruin HAR (2007) The energy balance experiment EBEX-2000. Part III: Behaviour and quality of the radiation measurements Bound-Lay Meteorol 123(1):55–75

Li SG, Eugster W, Asanuma J, Kotani A, Davaa G, Oyunbaatar D, Sugita M (2006) Energy partitioning and its biophysical controls above a grazing steppe in central Mongolia. Agric For Meteorol 137(1–2):89–106

Lloyd CR, Bessemoulin P, Cropley FD, Culf AD, Dolman AJ, Elbers J, Heusinkveld B, Moncrieff JB, Monteny B, Verhoef A (1997) A comparison of surface fluxes at the HAPEX-Sahel fallow bush sites. J Hydrol 189(1–4):400–425

Malhi Y, McNaughton K, Von Randow C (2004) Low Frequency Atmospheric Transport and Surface Flux Measurements. Lee X, Massman W, Law B, Handbook of Micrometeorology, pp 101–118

Massman WJ (2000) A simple method for estimating frequency response corrections for eddy covariance systems. Agric For Meteorol 104(3):185–198

Mauder M, Foken T (2006) Impact of post-field data processing on eddy covariance flux estimates and energy balance closure. Meteorol Z 15(6):597–609

McCaughey JH (1982) Spatial variability of Net radiation and soil heat flux density on two logged sites at Montmorency, Quebec. J Appl Meteorol 21(6):777–787

Moore CJ (1986) Frequency response corrections for eddy correlation systems. Bound-Lay Meteorol 37(1):17–35

Moore CJ, Fisch G (1986) Estimating heat-storage in Amazonian tropical forest. Agric For Meteorol 38(1–3):147–168

Nie D, Kanemasu ET, Fritschen LJ, Weaver HL, Smith EA, Verma SB, Field RT, Kustas WP, Stewart JB (1992) An intercomparison of surface-energy flux measurement systems used during FIFE 1987. J Geophys Res (A Atmospheres) 97(D17):715–724

Noormets A, Chen J, Crow TR (2007) Age-dependent changes in ecosystem carbon fluxes in managed forests in northern Wisconsin, USA. Ecosystems 10(2):187–203

Noormets A, Gavazzi MJ, McNulty SG, Domec JC, Sun G, King JS, Chen JQ (2010) Response of carbon fluxes to drought in a coastal plain loblolly pine forest. Global Change Biol 16(1):272–287

Oliphant AJ, Grimmond CSB, Zutter HN, Schmid HP, Su HB, Scott SL, Offerle B, Randolph JC, Ehman J (2004) Heat storage and energy balance fluxes for a temperate deciduous forest. Agric For Meteorol 126(3–4):185–201

Oncley SP, Foken T, Vogt R, Kohsiek W, DeBruin HAR, Bernhofer C, Christen A, van Gorsel E, Grantz D, Feigenwinter C, Lehner I, Liebethal C, Liu H, Mauder M, Pitacco A, Ribeiro L, Weidinger T (2007) The energy balance experiment EBEX-2000. Part I: Overview and energy balance. Bound-Lay Meteorol 123(1):1–28

Sanchez JM, Caselles V, Rubio EM (2010) Analysis of the energy balance closure over a FLUXNET boreal forest in Finland. Hydrol Earth Syst Sci 14(8):1487–1497

Schlesinger WH, Raikes JA, Hartley AE, Cross AF (1996) On the spatial pattern of soil nutrients in desert ecosystems. Ecology 77(4):1270–1270

Schmid HP (1997) Experimental design for flux measurements: matching scales of observations and fluxes. Agric For Meteorol 87(2–3):179–200

Shao CL, Chen JQ, Li LH, Xu WT, Chen SP, Gwen T, Xu JY, Zhang WL (2008) Spatial variability in soil heat flux at three Inner Mongolia steppe ecosystems. Agric For Meteorol 148(10):1433–1443

Shao CL, Chen JQ, Li LH, Zhang LH (2012) Ecosystem responses to mowing manipulations in an arid inner Mongolia steppe: an energy perspective. J Arid Environ 82:1–10

Shao CL, Chen JQ, Li LH (2013) Grazing alters the biophysical regulation of carbon fluxes in a desert steppe. Environ Res Lett 8:025012

Stannard DI (1997) A theoretically based determination of Bowen-ratio fetch requirements. Bound-Lay Meteorol 83(3):375–406

Stannard DI, Blanford JH, Kustas WP, Nichols WD, Amer SA, Schmugge TJ, Weltz MA (1994) Interpretation of surface flux measurements in heterogeneous terrain during the Monsoon'90 experiment. Water Resour Res 30(5):1227–1239

Turnipseed AA, Blanken PD, Anderson DE, Monson RK (2002) Energy budget above a high-elevation subalpine forest in complex topography. Agric For Meteorol 110:177–201

Twine TE, Kustas WP, Norman JM, Cook DR, Houser PR, Meyers TP, Prueger JH, Starks PJ, Wesely ML (2000) Correcting eddy-covariance flux underestimates over a grassland. Agric For Meteorol 103(3):279–300

van der Molen MK, Gash JHC, Elbers JA (2004) Sonic anemometer (co)sine response and flux measurement – II. The effect of introducing an angle of attack dependent calibration Agric For Meteorol 122(1–2):95–109

Webb EK, Pearman GL, Leuning R (1980) Correction of flux measurements for density effects due to heat and water-vapor transfer. Q J Roy Meteor Soc 106:85–100

Wilson KB, Goldstein A, Falge E, Aubinet M, Baldocchi D, Berbigier P, Bernhofer C, Ceulemans R, Dolman H, Field C, Grelle A, Ibrom A, Law BE, Kowalski A, Meyers T, Moncrieff J, Monson R, Oechel W, Tenhunen J, Valentini R, Verma S (2002) Energy balance closure at FLUXNET sites. Agric For Meteorol 113(1–4):223–243

Zhang WL, Chen SP, Chen J, Wei L, Han XG, Lin GH (2007) Biophysical regulations of carbon fluxes of a steppe and a cultivated cropland in semiarid Inner Mongolia. Agric For Meteorol 146(3–4):216–229

doi:10.1186/2192-1709-3-7
Cite this article as: Shao *et al.*: **Spatial variation of net radiation and its contribution to energy balance closures in grassland ecosystems.** *Ecological Processes* 2014 **3**:7.